Study of the Spin-Relaxation Times and the Effects of Spin-Exchange Collisions in an Optically Oriented Sodium Vapor*

L. WILMER ANDERSON AND ALAN T. RAMSEY
Department of Physics, University of Wisconsin, Madison, Wisconsin
(Received 19 April 1963)

The spin-relaxation time of an optically oriented sodium vapor diffusing in a helium or neon buffer gas has been measured and analyzed by the method of Franzen. The diffusion coefficients for sodium in helium and neon are 1.0 ± 0.3 and 0.50 ± 0.17 cm^2/sec, respectively. The disorientation cross sections for sodium colliding with helium and neon are $(3\pm4)\times10^{-26}$ and $(1.8\pm0.6)\times10^{-24}$ cm^2, respectively. The radio-frequency (rf) Zeeman transitions of the sodium atoms in the ground state have been examined. An analysis of the effects of spin-exchange collisions between sodium atoms on the intensities and line shapes of the various Zeeman transitions is presented. From these studies a spin exchange cross section of $(1–3)\times10^{-14}$ cm^2 is estimated for two sodium atoms colliding. The main source of error in this measurement is probably lack of knowledge of the sodium vapor pressure in the sodium-absorption cells.

I. INTRODUCTION

An optically oriented alkali-metal vapor provides a tool for examining the collisions of the alkali-metal atom with other atoms. The spin-relaxation time of the alkali metal vapor diffusing in a buffer gas can provide information on the collisions of the alkali metal with the buffer gas, and an examination of the rf Zeeman transitions between the ground-state sublevels of the alkali-metal atom can provide information on the spin-exchange collisions of two alkali-metal atoms.

The spin relaxation of an optically oriented rubidium vapor has been studied previously by several people.[1–4] Franzen measured the spin relaxation time for oriented rubidum in several buffer gases, neon, argon, krypton, and xenon.[1] Bernheim continued these studies on rubidium using helium as a buffer gas.[2] These experiments have shown that the spin-relaxation time of rubidium varies with the pressure of the buffer gas; initially increasing as the pressure increases, passing through a maximum, and then decreasing as the pressure increases further. The interpretation given by Franzen to these results was that at low buffer-gas pressures the buffer gas inhibited the diffusion of the rubidium to the wall of the container (every collision of a rubidium atom with the wall was assumed to disorient the atom) thus causing the initial rise in the relaxation time as a function of the buffer-gas pressure. The decrease in the spin-relaxation time at higher buffer-gas pressures is due to disorienting collisions of the rubidium with the buffer gas. It was found, also, that the maximum spin-relaxation time and the buffer gas pressure, at which this maximum occurs, are very dependent on which buffer gas was used. Noble gases with a low atomic number were found to have smaller cross sections for disorienting collisions with the rubidium than those of high atomic number. Bernheim has proposed a mechanism, which may explain these disorienting collisions. Other experiments yielding spin relaxation times of alkali metals have also been performed.[5,6]

Spin-exchange collisions between two atoms containing unpaired electron spins have been examined by a number of people. Purcell and Field, and Wittke and Dicke have given theoretical analyses of such collisions.[7,8] Optical pumping experiments involving spin-exchange collisions have been reported. These experiments have used the spin-exchange collisions to orient atoms and even free electrons, which cannot be oriented by the direct pumping process, and these experiments have been used to study the effect of spin-exchange collisions on the linewidths and intensities of the rf transitions of the optically oriented atoms.[9–16]

* This research was supported initially by a grant from the Research Corporation and later by a grant from the National Science Foundation.

[1] W. Franzen, Phys. Rev. **115**, 850 (1959).
[2] R. Bernheim, J. Chem. Phys. **36**, 135 (1962).
[3] M. Bouchiat and J. Brossel, Compt. Rend. **254**, 3829 (1962).
[4] R. Brewer, J. Chem. Phys. **37**, 2504 (1962).
[5] H. G. Dehmelt, Phys. Rev. **105**, 1487 (1957). In this pioneering study of the spin-relaxation times of alkali metals in buffer gases, Dehmelt first showed that long spin-relaxation times could be obtained for Na diffusing in Ar. From the measured relaxation times of 0.02 sec in Ar at a pressure of 40 cm of Hg in a 0.1 liter cell and 0.2 sec in Ar at a pressure of 3 cm of Hg in a 1 liter cell, one can estimate that the diffusion constant of Na in Ar is $D_0\sim0.2$ cm^2/sec and the disorientation cross section is $\sigma\sim5\times10^{-23}$ cm^2. These values are quite consistent with the measurements reported in this paper and with the measurements reported in Refs. 1 and 2.
[6] L. W. Anderson and A. T. Ramsey, Phys. Rev. **124**, 1862 (1961).
[7] E. M. Purcell and G. B. Field, Astrophys. J. **124**, 542 (1956).
[8] J. P. Wittke and R. H. Dicke, Phys. Rev. **103**, 620 (1956).
[9] L. W. Anderson, F. M. Pipkin, and J. C. Baird, Phys. Rev. **116**, 87 (1959).
[10] L. W. Anderson, F. M. Pipkin, and J. C. Baird, Phys. Rev. **120**, 1279 (1960).
[11] H. G. Dehmelt, Phys. Rev. **109**, 381 (1958). In this important paper, spin-exchange collisions of free electrons with optically oriented sodium are used to orient the electrons and are used to detect the magnetic resonance of the electrons. The effect of heating up the electron-spin system is reflected in the subsequent heating of the sodium-spin system. This is, of course, very similar to the results obtained in this paper which show that any pair of levels in the sodium spin system are coupled to all the other levels by spin-exchange collisions. Similar results are obtained in Refs. 10, 12, and 16.
[12] R. Novick and H. E. Peters, Phys. Rev. Letters **1**, 54 (1958).
[13] M. Arditi and T. R. Carver, Phys. Rev. **109**, 1012 (1958).
[14] W. W. Holloway, E. Lusher, and R. Novick, Phys. Rev. **126**, 2109 (1962).
[15] R. H. Lambert and F. M. Pipkin, Phys. Rev. **128**, 198 (1962).
[16] P. Franken, R. Sands, and J. Hobart, Phys. Rev. Letters **1**, 52 and 188E (1958).

The first part of this paper contains a description of the measurement of the spin-relaxation time of sodium as a function of the density of the buffer gas using helium and neon as buffer gases. The second part of this paper makes use of these measured relaxation times to study the effect of spin-exchange collisions on the optical pumping process and state populations.

II. THE SPIN-RELAXATION TIME OF AN OPTICALLY ORIENTED SODIUM VAPOR

A. Method

The spin-relaxation time of a sodium vapor has been measured by the method introduced by Franzen.[1] A sodium vapor, contained in a spherical cell with a buffer gas was oriented by illuminating the vapor with circularly polarized resonance radiation (only the D_1 line of the sodium doublet was used).[17] The sodium vapor absorbs circularly polarized resonance radiation and re-emits radiation of a different polarization so that a net angular momentum is transferred to the sodium vapor. In the steady state the light provides the same amount of angular momentum to the sodium as the sodium loses in collisions with the wall and the buffer gas. The sample becomes more transparent as it becomes polarized so that the transmission of the resonance radiation by the cell may be used to monitor the polarization of the sample.

After the system has reached a steady state the resonance radiation is blocked off and the polarization is allowed to decay in the dark. The decay of the polarization is measured as a function of time by observing the transparency of the cell after various dark times.

In this experiment the light transmitted through the absorption cell is monitored by a photocell. In the steady state the photocell draws a current proportional to the transmitted light. When the light beam is interrupted by the shutter, the photocurrent drops abruptly to zero. The photocurrent remains zero while the polarization of the sample decays. When the light is again permitted to pass through the cell the photocurrent immediately increases to a value corresponding to the transmission of the depolarized cell. As the light slowly pumps the system back to the steady state the photocurrent increases until equilibrium is reached. The photocurrent passes through a resistor providing a voltage which is displayed on an oscilloscope. These oscilloscope traces provide a measurement of the transparency of the cell as a function of the time the shutter is closed.

B. Experimental Apparatus

A block diagram of the experimental apparatus is shown in Fig. 1. A sodium lamp, a G.E. Na1, was enclosed in a thermostatically controlled oven and was run from batteries. An electronic regulator maintained the

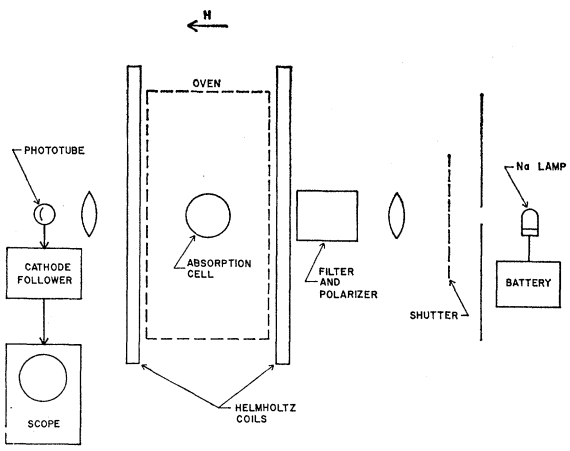

FIG. 1. The block diagram of the experimental apparatus.

current through the lamp at a constant level, usually 3.5 A. The shutter was a simple photographic type manufactured by Packard, with an aperture of 1.75 in. It was modified to open and close with a hand-operated lever. The opening and closing times were about 25 msec each. After passing through the shutter the light was collimated by a lens and directed through a Lyot polarization filter tuned to pass the D_1 line (the $3\,^2P_{1/2}$–$3\,^2S_{1/2}$ transition) and eliminate the D_2 line (the $3\,^2P_{3/2}$–$3\,^2S_{1/2}$ transition). The light was then circularly polarized by a quarter wave plate. After passing through the absorption cell the light was focused by a lens onto the cathode of a 929 phototube. The output of the phototube was fed into a cathode follower and then into a Tektronix 560 oscilloscope with a type-63 vertical amplifier. All units were dc coupled. For some absorption cells the signals were only about one percent of the total transmitted light. The sensitive scales of the oscilloscope used to observe these signals were overloaded when the light was blocked off. In order to avoid this problem a mechanical switch was attached to the shutter. The switch grounded the oscilloscope input while the shutter was closed. The dc level of the cathode follower output was adusted so that grounding the oscilloscope input gave a signal which reliably triggered the oscilloscope. This switch was used only when necessary (e.g., for absorption cells where the spin-relaxation time was very short).

The absorption cell was located at the center of two pairs of Helmholtz coils. The larger pair had a diameter of 32 in. and was used to produce a static magnetic field parallel to the light beam. This magnetic field was usually between 10 and 14 G. When observing the Zeeman transitions in sodium (as described in the latter part of the paper), the magnetic field was swept linearly over the resonances by an electronic modulator driven by the saw tooth voltage from the oscilloscope horizontal deflection plates. The second pair of coils, which was at right angles to the first, was 6 in. in diameter and

[17] W. Franzen and A. G. Emslie, Phys. Rev. **108**, 1453 (1957).

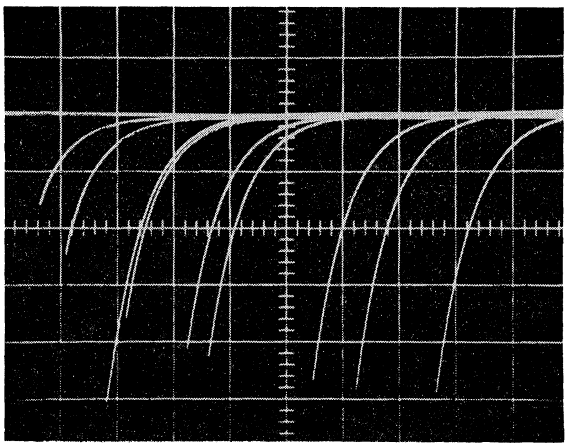

FIG. 2. The decay of the cell transparency. Time increases from left to right in units of 500 msec/div. The photocell output increases from bottom to top in units of 50 mV/div. The long trace two units from the left is a reference showing the transparency of an unpolarized cell. This picture was taken with the cell at a temperature of 173°C and using a cell whose density was 1.63×10^{19} He atoms/cc.

was used to supply the rf magnetic field to induce the Zeeman transitions. The rf coils were driven by a General Radio 805C oscillator.

The spherical absorption cells were made from half-liter round-bottom Pyrex flasks. The necks of the flasks were drawn off and two pumping leads were attached to the flasks, one for evacuating the flask and the other so that sodium could be distilled into the cell. No effort was made to clean the cells other than outgassing them with a torch when they were connected to the vacuum system. When the cell was evacuated and well outgassed, sodium was distilled into the cell and condensed onto a small patch of glass. A thermocouple in contact with this part of the cell gave the temperature of the cell.

After the sodium was distilled into the cell, the cell was filled with buffer gas to the desired pressure through the pumping lead. The cell was then sealed off and removed from the system. The buffer gas pressure was measured with a mercury manometer.

For pressures up to 50 cm of Hg at room temperature, the cells were filled from one liter flasks of spectroscopic gas supplied by Linde or Airco. For filling helium cells above this pressure, Bureau of Mines grade A well helium was used. This helium was purified in the following manner. Under high vacuum a layer of titanium was evaporated onto the walls of a 2-liter glass bulb. Helium was then admitted into this bulb filling it to a pressure of 2 atm at room temperature. There was a titanium filament in the bulb, which served two purposes. When heated, it set up convection currents in the bulb which greatly speeded the process of moving the impurities in the helium to the wall of the bulb where they could combine with or be adsorbed by the cool titanium surface. It, also, aided purification by combining directly with oxygen and nitrogen which came into contact with the hot filament. This purification was intended to remove oxygen, hydrogen, nitrogen, water, and carbon dioxide.

The absorption cells were heated to an operating temperature (about 150°C) in an oven made of $\frac{1}{2}$-in. plywood with 3 in. of mineral insulation. This oven had double windows on opposite sides so that the light could pass through. The oven was heated electrically. If the heater was turned off the initial rate of temperature fall from 150°C was $\frac{1}{2}$°C/min.

C. Data and Analysis

For an absorption cell at a given buffer-gas density the data taken on the spin-relaxation time consist of a photograph of a series of oscilloscope traces as shown in Fig. 2. The vertical scale is proportional to the intensity of light transmitted through the cell and the horizontal scale is proportional to the time measured from the closing of the shutter, which cuts off the light incident on the cell. The sweep of the oscilloscope is triggered when the shutter closes. When the transmitted light intensity falls to zero as the shutter interrupts the light beam, the oscilloscope trace drops abruptly to a voltage lower than shown on the photograph and moves in the direction of increasing time. The polarization of the sample is decaying in the dark, and the sodium vapor is becoming more absorbing. When the shutter reopens the trace moves quickly (too rapidly to register on the

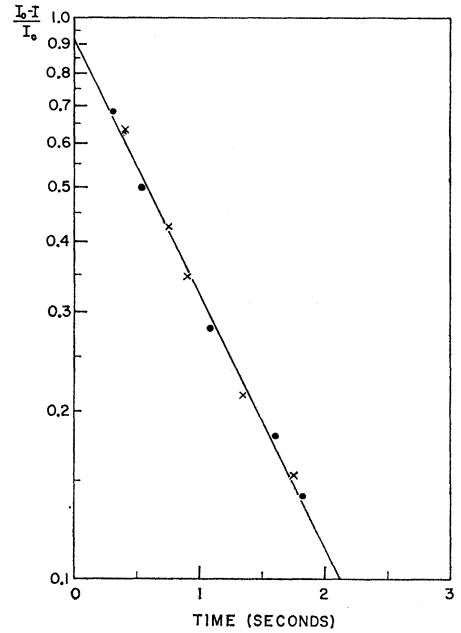

FIG. 3. A plot of $(I_0-I)/I_0$ versus time on semilog paper. The decrease of the transparency, I, of the cell as a function of time was taken from the picture of Fig. 2 and another picture of the same cell. I_0 is the decrease in the transparency of the cell from a polarized cell to a completely unpolarized cell. These data were taken using a cell whose density was $1.63 \times 10^{+19}$ He atoms/cc. The temperature of the cell was 173°C.

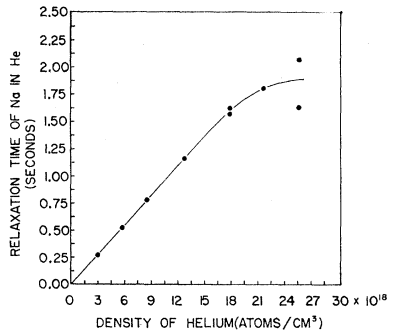

FIG. 4. The spin-relaxation time of optically oriented sodium diffusing in a He buffer gas as a function of He density. The first five data points (including the lower point at about 16.5×10^{18} atoms/cc) were obtained from cells filled with spectroscopic He. The four points at higher density were obtained from cells filled with purified mine He. The temperature of the cell was 154°C. The data show relatively large errors as indicated by the two points at 2.4×10^{19} atoms/cc. The solid curve is a fit to the data and not based on a theoretical form. A curve based on the theoretical form for the slowest mode was not used because of the uncertainty in σ for He. The values for the density of helium shown on the abscissa of the graph should be multiplied by 0.93.

photograph) to a value indicating the increased absorption of the cell and then rises slowly to its original level as the light again polarizes the sample. On the photograph in Fig. 2 a number of these traces have been superimposed. The long trace near the center of the picture is a reference value taken after the cell had been in the dark for a time long compared to the decay time. A curve drawn through the ends of the traces gives the decay of the transparency of the sodium vapor as a function of time and the reference value provides a measurement of the transparency of the unpolarized cell. The curve representing the transparency of the sodium vapor as a function of the time the shutter is closed is taken to be proportional to the decay of the polarization of the sample. This assumption is discussed in the Appendix. The decrease in the transparency of the cell is assumed to follow the exponential law $I=I_0(1-e^{-\lambda t})$, where I is the decrease in the transparency of the cell and I_0 is the decrease in the transparency of the cell from the steady-state value to the value for an unpolarized cell. Figure 3 shows a plot of $\ln[(I_0-I)/I_0]$ versus t. The slope of this line is the relaxation time.

The intercept for $t=0$ of the curve in Fig. 3 is not $(I_0-I)/I_0=1$. This may be due to the effect of the other modes of decay as discussed by Bernheim[2] or it may be due to the fact that our measured zero of time is not the exact time when the shutter closed since the triggering of the oscilloscope sweep was sometimes slightly different than the closing time of the shutter.

The data shown in Figs. 4 and 5 are the relaxation times of sodium in helium and neon, respectively, as a function of buffer-gas density.

The errors in these measurements were quite large as is shown in Fig. 4 by the two values of the spin-relaxation time for the cell whose density was about 2.36×10^{19} helium atoms/cc. One reason for these errors was the low light intensity. This low light intensity was caused by the small acceptance angle of the Lyot filter. Other sources of errors have not been investigated.

The data were analyzed in a manner similar to that used by Franzen.[1] Two modes of polarization decay were considered. In the first, a sodium atom which collides with the absorption cell wall is assumed to come off the wall with an equal probability of being in any of the eight magnetic sublevels of the ground state, and thus to have no polarization. In the second mode there may be a transfer of angular momentum between the interatomic orbital angular momentum and the spin of the sodium atom during the collision of a sodium atom and a buffer gas atom. In this analysis, this process is characterized by a cross section σ for a collision, from which the sodium atom emerges with an equal probability of being in any of the sublevels of the ground state. The equation governing the polarization of the atoms in the absence of light is then (see the Appendix)

$$dP/dt=D\nabla^2P-\bar{v}_{\rm rel}\sigma NP,$$

where D is the diffusion constant of the sodium in the buffer gas and N is the density of the buffer gas. A solution of this equation satisfying the boundary condition that the polarization be zero at the walls of the spherical cells is

$$P=\sum_{l,m,p} a_{l,m,p}\frac{J_{l+1/2}(pr)}{r^{1/2}}Y_l^m(\vartheta,\varphi)\times\exp[-(p^2D+N\bar{v}_{\rm rel}\sigma)t],$$

where l and m are integers and the summation of p is over the positive roots of $J_{l+1/2}(pR)=0$, where R is the radius of the cell. Since this is the solution of a diffusion equation, there is no single characteristic lifetime. The

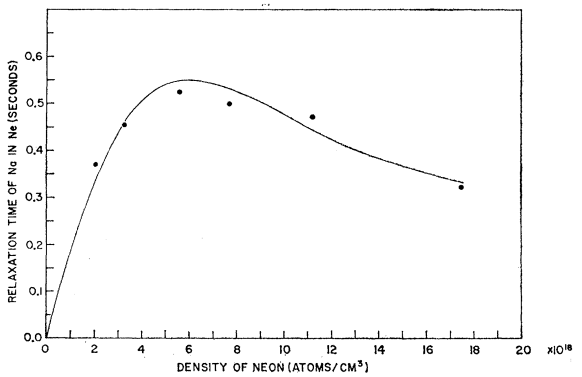

FIG. 5. The spin-relaxation time of optically oriented sodium diffusing in a neon buffer gas as a function of neon density. The temperature of the cell was 152°C. The solid curve is based on the theoretical form for the slowest relaxation curve and may be obtained by using the parameters in Table I. The values for the neon density shown on the abscissa of the graph should be multiplied by 0.93.

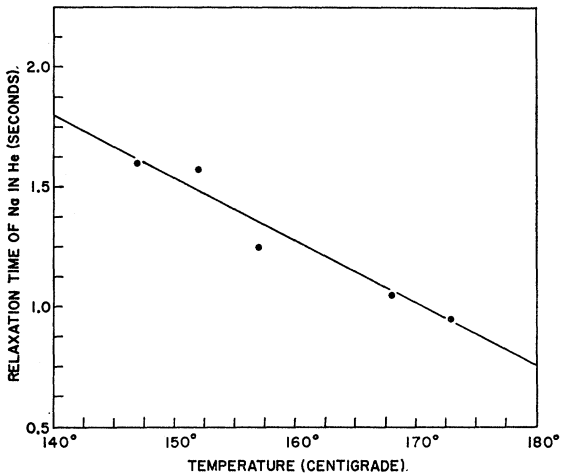

FIG. 6. The variation of the spin relaxation time of Na in a He buffer gas as a function of cell temperature. These data were obtained on a cell whose density was 1.63×10^{19} He atoms/cc. Over this temperature range the density of Na atoms increases by a factor of seven.

lifetime of the slowest mode, using $R=5$ cm is

$$T=\{0.395D_0(\rho_0/\rho)+N_0\sigma\bar{v}_{\rm rel}(\rho/\rho_0)\}^{-1},$$

where ρ is the density of the buffer gas and the subscript zeros refer to atmospheric pressure. In order to determine the parameters D_0 and σ this equation was fitted to the relaxation time versus buffer-gas density data of Figs. 4 and 5. The values of the parameters for these curves are given in Table I.

The relaxation times were measured at 154±2°C for helium and 152±2°C for neon. The temperature of the cell is important. Figure 6 shows the variation of the relaxation time as a function of temperature for a helium cell the density of which is 1.63×10^{18} atoms/cc. Simultaneous measurements of the relaxation time on a cell, whose density was 2.36×10^{19} atoms/cc, and the magnitude of the sodium polarization (see the discussion of the measurement of the sodium polarization in the next section) over the temperature range of 140 to 180°C showed no significant change in the polarization although the relaxation time apparently varied from 2.2 sec to about 1.2 sec. The interpretation given these results is that the apparent change in the spin-relaxation time is primarily due to the rapidly changing sodium vapor pressure in the cell, which alters the initial distribution of the polarized atoms in the cell. This causes modes other than the slowest to be important (e.g., if the polarized atoms are formed mostly near the front of the cell, as may be the case if the sodium atom density is high and the cell is not optically thin, then the polarized atoms can diffuse to the wall more rapidly than if they are created at the center of the cell).

TABLE I. The values of D_0, the diffusion constant for sodium in the buffer-gas helium or neon at a density of 2.45×10^{19} atoms/cc, and σ, the disorientation cross section.

Buffer gas	Temp (°C)	D_0 (cm²/sec)	σ (cm²)
Helium	154±2	1.0 ±0.3	$(3\pm4)\times10^{-26}$
Neon	152±2	0.50±0.17	$(1.8\pm0.6)\times10^{-24}$

III. THE EFFECTS OF SPIN EXCHANGE COLLISIONS ON THE OPTICALLY ORIENTED SODIUM VAPOR

In addition to collisions with the buffer gas and the absorption-cell wall, a sodium atom can collide with another sodium atom and during the collision exchange electron-spin coordinates with the other atom. The following analysis of the spin exchange collisions is similar to that given by Wittke and Dicke, and Purcell and Field.[7,8] When two sodium atoms collide they form a sodium molecule in one of two electronic states $^1\Sigma$ or $^3\Sigma$ depending upon whether the electron spins combine in a singlet or a triplet state. These two states, having very different interaction potentials, will evolve at different rates during a collision. The difference in phase between the singlet and triplet parts of the wave function after a collision is

$$\phi_{ts}=\int\frac{(V_t-V_s)dt}{\hbar},$$

where V_t and V_s are the interaction potentials of the triplet and singlet states and where the integral is taken over the time of the collision. Consider the situation where one sodium atom is at rest and another sodium atom is incident on the first with an energy E and an impact parameter b. When the atoms are far apart they are each represented by the quantum numbers J, I, F, m_F. As the atoms collide the total electronic-spin angular momentum of the pair becomes the good quantum number and the singlet and triplet parts of the initial wave function evolve with different phases. Thus after the collision the final wave function of the system is given by

$$\psi_f=(P_0+e^{-i\phi_{ts}}P_1)\psi_i(F_1,m_1;F_2,m_2),$$

where P_0 and P_1 are the projection operators for total spin angular momentum 0 and 1, respectively, and where the subscripts 1 and 2 refer to the two sodium atoms. The relative phase ϕ_{ts} is a rapidly varying function of E and b for a collision in which the atoms interact strongly. Thus an average is taken over ϕ_{ts} ultimately. The cross section for a "strong collision" (one for which $\phi_{ts}\gg1$) is given by

$$\sigma=\sigma_0[|(F_1',m_1';F_2',m_2'|P_0+e^{-i\phi_{ts}}P_1|F_1,m_1;F_2,m_2)|^2]_{\text{av over }\phi_{ts}},$$

where σ_0 is the geometrical area in the cross section. In this type of collision the total Z component of angular momentum of the two atoms is a constant of the motion. Thus, the polarization of the sample is not destroyed by spin-exchange collisions but instead is merely redistributed.[9]

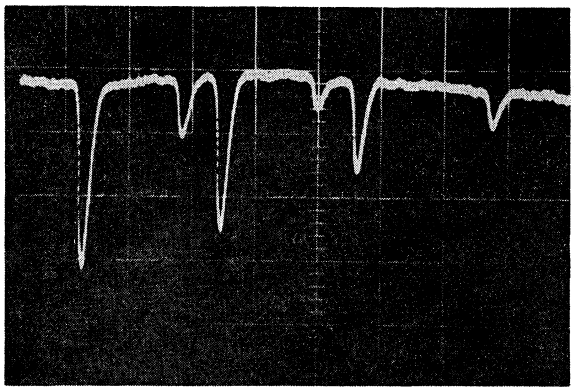

FIG. 7. The rf-induced Zeeman transitions in a polarized Na sample. The magnetic field increases from left to right at a rate of 5 sec/div. The output of the photocell increases from bottom to top in units of about one mV/div. The rf field was small enough that saturation was negligible. The oscillator frequency was approximately 9.8 Mc/sec. The cell used had a density of 1.15×10^{19} He atoms/cc and the temperature was 135°C.

It has been shown previously that if the time between spin-exchange collisions is short compared to either the spin-lattice relaxation time or the pumping time for the system then the effect of the spin-exchange collisions is to bring the state populations into the most probable distribution of atoms with a given total angular momentum along the axis of quantization. Such a set of state populations is given by $n_i=Ce^{-m_i\beta}$, where n_i is the population of the sublevel i of the ground state, C is a normalization constant, m_i is the Z component of total angular momentum of the sublevel i, and β is determined by the total polarization of the sample.[9]

An investigation of the Zeeman rf transitions ($\Delta F=0$, $\Delta m=\pm1$) has been carried out in optically oriented sodium. The apparatus was described earlier in this paper, and it was the same as was used for the measurement of spin-relaxation time except that the static magnetic field was modulated, and a rf magnetic field perpendicular to the static field was used to induce the transitions. At resonance the difference in state populations was reduced by the rf transitions and the transparency of the cell altered so that the transmitted light could be used to detect the resonance.

In order to obtain the relative state populations from measurements on the Zeeman transitions it is necessary to know how the measured change in transmitted light intensity at resonance depends on the state populations.

TABLE II. The values of the square of the matrix element $|(F,m|J_-|F,m+1)|^2$.

F,	$m+1$	F,	m	$\lvert(F,m\lvert J_-\rvert F,m+1)\rvert^2$
2,	2	2,	1	2
2,	1	2,	0	3
2,	0	2,	−1	3
2,	−1	2,	−2	2
1,	1	1,	0	1
1,	0	1,	−1	1

The decrease in the transparency of the optically oriented sodium cell as the magnetic field is swept slowly through a Zeeman resonance is

$$\Delta I\propto g_J^2\mu_0^2H_1^2|(F,m|J_-|F,m+1)|^2g(\nu)\Delta n\left(\frac{\partial I}{\partial(\Delta n)}\right),$$

where g_J is the electron g factor, μ_0 is the Bohr magneton, H_1 is circular component of the rf magnetic field, J is the electronic angular momentum, $g(\nu)$ is the line shape, Δn is the difference in populations between the states $|F,m)$ and $|F,m+1)$, and $\partial I/\partial(\Delta n)$ is the rate of change of the transmitted light intensity as a function of the difference of the state populations. This expression is merely the transition probability times the difference in state populations times the rate of change of light intensity per unit of change in the state population difference. This expression is valid if the rf magnetic field is small enough that saturation is negligible. If one assumes that $\partial I/\partial(\Delta n)$ has the same value no matter which states are involved in the rf transitions, then the change in light intensity as the magnetic field passes through a resonance is proportional to $|(F,m|J_-|F,m+1)|^2g(\nu)\Delta n$. In this study of the Zeeman transitions the line shape $g(\nu)$ of each of the transitions was determined by magnetic field inhomogeneity and, consequently, the line shape was the same for all six Zeeman transitions. The squares of the matrix elements $|(F,m|J_-|F,m+1)|^2$ are easily calculated and are given in Table II. The only remaining property affecting the intensity of the signals is Δn. In the case where $n_i=Ce^{-m_i\beta}$ it is obvious that $\Delta n=C[e^{m_i\beta}-e^{(m_i-1)\beta}]$.

Sodium, having a $^2S_{1/2}$ ground state and a nuclear spin $\frac{3}{2}$, has five magnetic sublevels in the $F=I+J=2$ hyperfine level and three magnetic sublevels in the $F=1$ level of the ground state. There are six Zeeman transitions ($\Delta F=0$, $\Delta m=\pm1$) among these eight sublevels. At a sufficiently large magnetic field all six transitions are resolved.

The Zeeman resonances in sodium were first studied in a cell in which the measured spin relaxation time was about one second. This cell had a helium buffer gas density of 1.15×10^{19} atoms/cc. As can be seen from Fig. 2 the time required for the light to pump a cell from an unpolarized state into a steady state of polarization was about $\frac{1}{2}$ sec. The spin-exchange collision time depends on the sodium-atom density but in all cases studied here was much shorter than 50 msec. Thus, the state populations might be expected in this case to be given quite accurately by $n_i=Ce^{-m_i\beta}$.

Figure 7 shows an oscilloscope picture of the six Zeeman transitions in the cell described above. Table III gives the measured intensities of these Zeeman transitions and compares these measurements with the intensities expected in a cell for which $e^{-\beta}=1.8$ and $\beta=-0.6$. The agreement is remarkable. In other cells values of β as large as 0.7 have been observed. These measurements yield a polarization, $P=\langle m\rangle=\sum_i m_in_i$

TABLE III. Table of Zeeman rf transition intensities. The measured intensities are in arbitrary units. The calculated intensities are normalized so that the calculated intensity for the transition $F=2, m=-2 \leftrightarrow F=2, m=-1$ is the same as the measured intensity for this transition. The value $e^{-\beta}=1.80$ has been used in the calculated intensities.

Transition $F, m-1 \leftrightarrow F, m$	Calculated intensity $\lvert(F, m-1 \lvert J_- \rvert F,m)\rvert^2 \times[e^{-m\beta}-e^{-(m-1)\beta}]$	Measured intensity
$2, -2 \leftrightarrow 2, -1$	$2\times1.4 = 2.8$	2.8
$2, -1 \leftrightarrow 2, 0$	$3\times0.78 = 2.4$	2.4
$2, 0 \leftrightarrow 2, 1$	$3\times0.43 = 1.3$	1.3
$2, 1 \leftrightarrow 2, 2$	$2\times0.24 = 0.48$	0.5
$1, -1 \leftrightarrow 1, 0$	$1\times0.78 = 0.78$	0.8
$1, 0 \leftrightarrow 1, 1$	$1\times0.43 = 0.43$	0.4

$=0.83$ and correspond to 32% of the atoms in the state $F=2$, $m=2$. The polarization of the electronic spin, S, is about 30%. Thus, the sodium vapor in this case is described by a single parameter, a spin temperature, which is the same in magnitude for all eight sublevels, but which is positive for the $F=2$ hyperfine level and negative for the $F=1$ hyperfine level.[18]

The quantity $\partial I/\partial(\Delta n)$ has been assumed to have the same value no matter which levels are involved in the rf transitions. This assumption is true in two cases, which will be discussed. Suppose that the optically pumped system is such that the spin-relaxation time and the pumping time are both much greater than the spin-exchange collision time so that the state populations are given by $n_i=Ce^{-m_i\beta}$. The polarization of the sample $P=\sum_i m_i n_i$ and the absorption of the cell $K=\sum_i AP_i n_i$ are functions only of β. A is a constant proportional to the light intensity and P_i is the relative absorption of light by the sublevel i of the ground state. Table IV gives the values of P_i. Although this equation for the absorption of the cell assumes that the light has the same intensity for each hyperfine component and that the cell is optically thin, the fact that the absorption K is a function only of β is valid if the cell is optically thin for any spectral distribution of the incident light. Since I, the transmitted light intensity, is just the incident light intensity minus K, the absorbed light, I is, also, a function only of β. Therefore, $\partial I/\partial(\Delta n)=(dI/dP)dP/d(\Delta n)$. Since $P=\sum_i m_i n_i$, it follows that $\Delta P=m_i\Delta n_i+m_j\Delta n_j$, where the rf transitions are induced between the sublevels i and j of the ground state. Because the transition probabilities for induced emission and absorption are the same $\Delta n_i=-\Delta n_j$ and $\Delta P=\Delta n_i(m_i-m_j)$. For the Zeeman transitions $m_i-m_j=1$. Since $\Delta n=n_i-n_j$ it follows that $\Delta(\Delta n)=\Delta n_i-\Delta n_j=2\Delta n_i$ and thus $dP/d(\Delta n)=\frac{1}{2}$. Hence, $\partial I/\partial(\Delta n)=\frac{1}{2}dI/dP$ and does not depend upon which two levels i and j are involved in the rf transitions. In general, the population of the eight sublevels of the ground state cannot be written in terms of only one parameter. In the general case,

$$\frac{\partial I}{\partial(\Delta n)}=\sum_i \frac{\partial I}{\partial n_i}\cdot\frac{\partial n_i}{\partial(\Delta n)}$$

may depend upon which sublevels are involved in the rf transitions. The other case where $\partial I/\partial(\Delta n)$ is independent of the levels, connected by the rf transitions, is the case when the spin exchange collision time is very long and the change in the population of two levels does not change the other populations. In this case $\Delta I=\Delta n_i P_i+\Delta n_j P_j=\Delta n_i(P_i-P_j)$. For the Zeeman transitions $\Delta m=\pm1$ and $\lvert P_i-P_j\rvert=1$ as can be seen from Table IV. In this case $\partial I/\partial(\Delta n)=\frac{1}{2}$ and is independent of the two levels in Δn. The sign of $\partial I/\partial(\Delta n)$ is plus for the Zeeman transitions in the $F=2$ state and minus for the Zeeman transitions in the $F=1$ state. The significance of this difference in sign for $\partial I/\partial(\Delta n)$ is that the optical pumping process tends to populate the magnetic sublevels with the highest m value in the $F=2$ state and those with the lowest m level in the $F=1$ state.

All the changes in the intensity of the transmitted light discussed so far have been decreases in the transmitted light as the magnetic field sweeps across the resonance. This is obvious in the situation where the spin exchange collision time is long compared to the pumping time or the spin-relaxation time since the most absorbing levels are depopulated by the light and the least absorbing levels obtain an excess population.[5] However, when the spin-exchange collision time is short compared to the spin relaxation time, or the pumping time, the more absorbing magnetic sublevels in the $F=1$ state have larger populations than the less absorbing sublevels in the $F=1$ state.[6] The reason the resonance appears as a decrease in the transmitted light intensity is that the spin-exchange collisions couple all the levels together tightly and the rf transitions change

TABLE IV. The relative optical absorption probabilities, P_i, of the eight sublevels of the ground state of sodium. The resonance radiation incident on the cell is assumed to be left circularly polarized, to contain only the D_1 line ($3\,^2P_{1/2} \rightarrow 3\,^2S_{1/2}$), and to have the same intensity for each hyperfine state.

State (F,m)	P_i
2, 2	0
2, 1	1
2, 0	2
2, −1	3
2, −2	4
1, 1	3
1, 0	2
1, −1	1

[18] The state populations are given by $n_i=Ce^{-m_i\beta}$ so that the population of a sublevel is determined by m_i and is independent of the hyperfine level. The "spin temperature" is different in sign but has the same magnitude for the two hyperfine levels because the g factor is different in sign but has the same magnitude for the two hyperfine levels. It should also be noted that optically the least absorbing sublevels have the higher populations for the $F=2$ hyperfine level but that the most absorbing sublevels have the higher populations for the $F=1$ hyperfine level (see Table IV).

the populations of all eight magnetic sublevels in such a way as to give a net absorption of light.

Although cumbersome this discussion shows the validity of the assumption, which enabled us to obtain the state populations in the case where the spin-exchange collision time is short compared to the spin-relaxation time and the pumping time.

The discussion just completed on the evaluation of $\partial I/\partial(\Delta n)$ for the case where the spin-exchange collision time is very short compared to the spin-relaxation time and the pumping time was based on the assumption that the sweep of the magnetic field across the resonance was slow compared to all characteristic times of the system. Figure 8 shows the shapes of the resonance lines as a function of the sweep speed of the magnetic field. In Fig. 8(a) the sweep is very slow and all six transitions appear as a decrease in transmitted light intensity. However, as the sweep speed is increased [Figs. 8(b) and (c)] a "spike" corresponding to an increase in the transmitted light appears as the magnetic field begins to sweep across the two resonances $F=1$, $m=1 \leftrightarrow F=1$, $m=0$ and $F=1$, $m=0 \leftrightarrow F=1$, $m=-1$. The interpretation of this spike is that during the time before a spin-exchange collision has occurred the rf field has reduced the population difference between the two states and hence the transmitted light increases because initially the more absorbing level had a larger population than the less absorbing level. This spike is absent in the four transitions $F=2$, $m \leftrightarrow F=2$, $m=\pm 1$ because initially the more absorbing levels have lower populations, than the less absorbing levels. The width of this spike is equal to the average spin-exchange collision time.[19] The width of the spike has been measured as a function of the temperature and the results are shown in Fig. 9. The variation in the temperature causes the sodium vapor pressure to change. The sodium vapor pressure as a function of temperature was obtained from Ditchburn

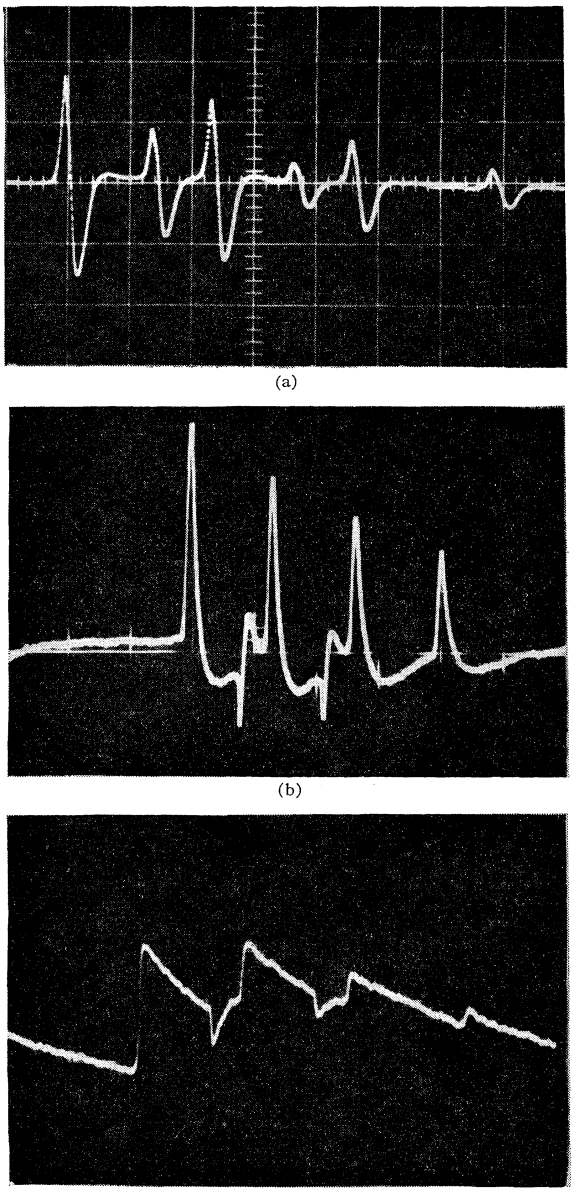

FIG. 8. The Zeeman transitions in polarized Na, showing the effect of the rate at which the magnetic field is swept across the resonance. The magnetic field increases from left to right. The oscilloscope was ac coupled to the photocell, giving a derivative-type line shape. Reading from the left, the second and fourth resonances are the Zeeman transitions in the $F=1$ hyperfine state. The sweep speed of the magnetic field for the three pictures was 2 sec/div for picture (a), 200 msec/div for picture (b), and 50 msec/div for picture (c). In picture (a) the resonances all have the same general shape of the absorption followed by an RC undershoot (increased absorption caused a bottom to top deflection of the trace). In picture (b) the two Zeeman resonances in the $F=1$ state have the initial spike of lower absorption followed by increased absorption. In picture (c) the sweep is rapid enough that the light does not pump the system back to equilibrium before the next resonance is reached. In picture (c) the two Zeeman resonances in the $F=1$ state correspond to lower absorption for the cell and the sweep is rapid enough that the shape of the spike is shown. The pictures (a), (b), and (c) are shown only to explain the effect and were not all taken on the same cell or at the same temperature.

[19] The "width of the spike" was taken as the time necessary for the light intensity to return to the same level as before the resonance was traversed. This width was taken as the average time between spin-exchange collisions. For the rapid sweeps (as shown in Fig. 8), the time spent crossing the resonance was quite short (as measured by the rapid change of the light intensity as the magnetic field reached the resonant condition). The slow decay on the trailing edge was due to the light repumping the system to equilibrium. For a sufficiently rapid sweep rate, the "width of the spike" on the two Zeeman transitions, in the $F=1$ level was greater than the width of the initial change of the light intensity as the resonant condition was reached and the width was independent of the sweep rate. This is consistent with the interpretation of this as a measure of spin-exchange time. Because of the difficulty of actually obtaining correct averages over thermal-velocity distributions these have not been successfully carried out by the authors. This and the fact that the shape of the "spike" at slow sweeps is distorted by spin-exchange collisions occurring during the time necessary to cross the line make this a method not suited for a precision determination of the spin-exchange cross section. However, the error introduced is probably not as large as that in the vapor pressure (see Ref. 20). (Note that for Fig. 8 the three pictures (a), (b), and (c) were all taken under very different conditions as far as rf field, static field, modulation width and relaxation time are concerned and are shown only in order to illustrate the method. Therefore, no conclusions can be made by comparing these pictures with each other.)

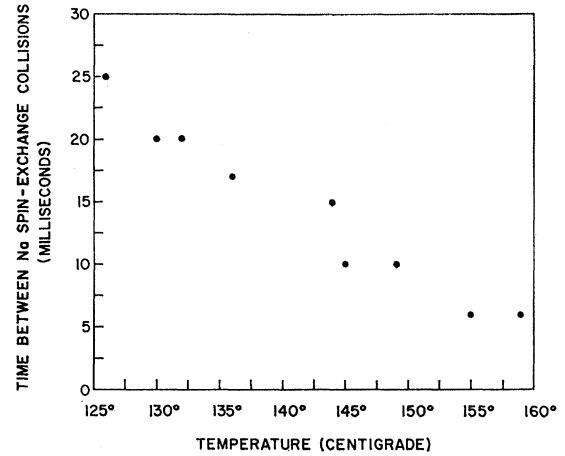

FIG. 9. The time between spin-exchange collisions in sodium measured as a function of the temperature of the absorption cell. The time was measured as the width of the spike in the rf Zeeman transitions in the $F=1$ state as described in the text.

and Gilmour.[20] A graph of the sodium vapor density versus temperature used in the calculations is shown in Fig. 10. The spin-exchange cross section was calculated assuming the time between spin exchange collisions T_2 was given by $T_2=1/n\sigma_0\bar{v}$. where n is the sodium atom density and $\bar{v}$ is the relative velocity of two sodium atoms. The values of the spin-exchange cross section are given in Table V. The error in the determination of the spin-exchange cross section by this method is probably due mainly to the error in the sodium vapor pressure.[21]

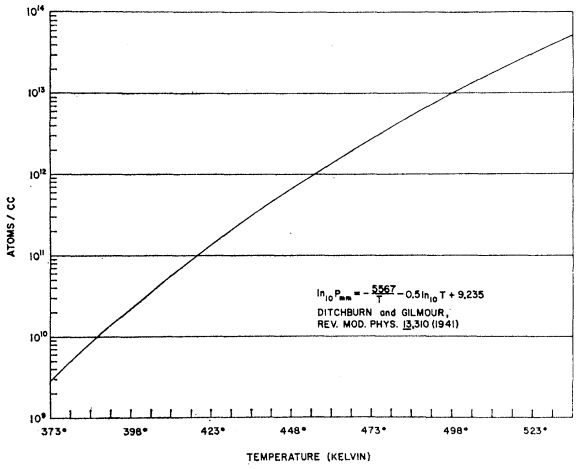

FIG. 10. The density of Na atoms in an absorption cell containing liquid Na as a function of the temperature of the cell. This curve was obtained by extrapolating the empirical formula for the Na vapor pressure as a function of temperature from the paper by R. W. Ditchburn and J. C. Gilmour (Ref. 18).

[20] R. W. Ditchburn and J. C. Gilmour, Rev. Mod. Phys. **13**, 310 (1941).

[21] P. Franken (private communication). Dr. Franken has reported privately to us that he has observed that the vapor pressure of sodium may depend on the past history of a cell as well as its temperature. It would be difficult to know the sodium-vapor pressure even if this were not the case since the data of Ditchburn and Gilmour was not taken at this low a temperature and so the vapor pressure used is an extrapolation of the measured vapor pressures.

TABLE V. The spin-exchange cross section, σ_0. The spin exchange cross section as measured from the line shapes in the rapid passage across the Zeeman resonances in the $F=1$ state.

Temp (°K)	σ_0[a,b] ($\times10^{-14}$ cm^2)	Temp (°K)	σ_0[a,b] ($\times10^{-14}$ cm^2)
399	1.95	418	1.22
403	1.72	422	0.95
405	1.53	428	0.99
409	1.31	432	0.75
417	0.87		

[a] Average $\sigma_0=1.3\times10^{-14}$ cm^2.
[b] The spin-exchange cross section as measured from the failure to observe a population difference between the three magnetic sublevels in the $F=1$ hyperfine level in a cell for which $T_1=16$ msec.
$\sigma_0=3\times10^{-14}$ cm^2.

However, it seems reasonable to state that the spin-exchange cross section is between $(1\text{–}3)\times10^{-14}$ cm^2.

The effects of saturation in an optically pumped system such as the one described are shown in Fig. 11. The interpretation of the results on the saturation measurements are that with a high enough rf magnetic field the entire polarization of the sample is destroyed when the static magnetic field sweeps across any one of the Zeeman transitions. This complete depolarization occurs because the spin-exchange collisions couple all eight of the levels together. Thus, all six of the Zeeman transitions have the same intensity if the rf magnetic field is sufficiently high.

It has been pointed out previously that if the spin-relaxation time and the spin-exchange collision time are about the same, then the population differences for the magnetic sublevels in the $F=1$ state of the optically oriented sodium will be much smaller than the population differences in the $F=2$ state, because the optical pumping process and the spin-exchange collisions will each tend to populate the same magnetic sublevels in the $F=2$ state, and the two processes will interfere in the $F=1$ state.[6] The relative populations have been measured previously and a value for the spin-exchange cross section has been derived from these populations and the measured spin-relaxation time.[6] These measurements were probably not accurate because the value of $\partial I/\partial(\Delta n)$ was assumed to be the same for each transition. The sweep speed was, also, very rapid compared to the spin-exchange collision time as is clear since the transitions $F=1$, $m\leftrightarrow F=1$, $m\pm1$ corresponded to an increase in the transmitted light intensity. In the present studies on sodium, a number of cells have been examined and the interference of the two processes in the $F=1$ state populations has been verified. In particular, Fig. 12 shows the rf transitions with a large amplitude rf magnetic field and with a slow sweep of the static field in a helium cell whose density was 1.62×10^{17} atoms/cc. The spin-relaxation time of this cell is about 16 msec, as estimated from Fig. 4. The four Zeeman transitions

$F=2$, $m \leftrightarrow F=2$, $m\pm1$ are clearly visible, but the two Zeeman transitions $F=1$, $m \leftrightarrow F=1$, $m\pm1$ are smaller than the noise. The interpretation of this is that in this cell the interference is complete and $\Delta n=0$ for the $F=1$ magnetic sublevels. The populations for the eight magnetic sublevels have been calculated previously. These

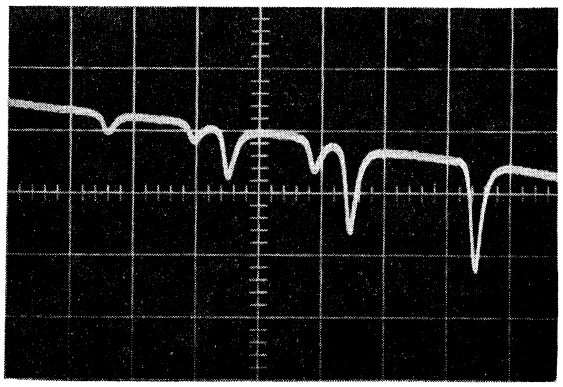

(a)

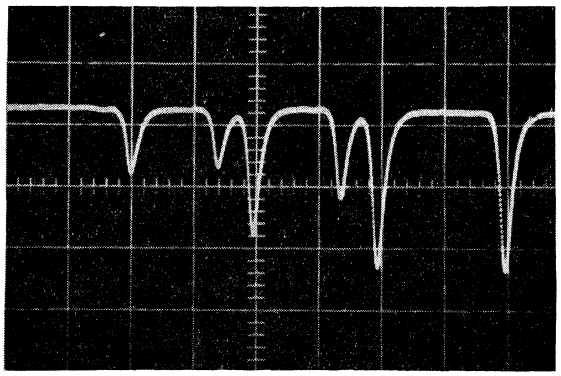

(b)

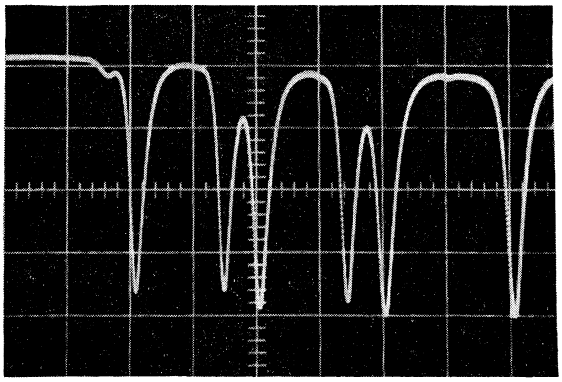

(c)

FIG. 11. The effect of the magnitude of the rf magnetic field on the Zeeman transition in polarized Na. The rf voltage levels as measured at the generator were in the ratio 1:4:8 for pictures (a), (b), and (c), respectively. The signal strength increases with the rf level; the vertical scales were 2, 2, and 5 mV/div for pictures (a), (b), and (c), respectively. These pictures were taken using a cell whose density was 2.4×10^{19} He atoms/cc and whose temperature was 195° C. The sweep speed of the static magnetic field was 5 sec/div.

TABLE VI. The state populations of Na.[a]

F	m	Population
	2	$\frac{1}{8}+\alpha^{b,e}$
	1	$\frac{1}{8}+\beta^{c,e}$
2	0	$\frac{1}{8}$
	−1	$\frac{1}{8}-\beta^{c,e}$
	−2	$\frac{1}{8}-\alpha^{b,e}$
	−1	$\frac{1}{8}-\delta^{d,e}$
1	0	$\frac{1}{8}$
	+1	$\frac{1}{8}+\delta^{d,e}$

[a] For the conditions when these solutions are valid see Ref. 6.

[b] $\alpha=A\dfrac{64/T_1^2+44/T_1T_2+7.6/T_2^2}{(8/T_1+2.78/T_2)(32/T_1^2+16.5/T_1T_2)}$.

[c] $\beta=A\dfrac{32/T_1^2+27.6/T_1T_2+3.8/T_2^2}{(8/T_1+2.78/T_2)(32/T_1^2+16.5/T_1T_2)}$.

[d] $\delta=-A\dfrac{32/T_1^2+5.4/T_1T_2-3.8/T_2^2}{(8/T_1+2.78/T_2)(32T_1+16.5T_1T_2)}$.

T_1 is the spin-relaxation time and $T_2=\dfrac{1}{\langle nv_{\mathrm{rel}}\sigma_0\rangle_{\mathrm{av}}}$.

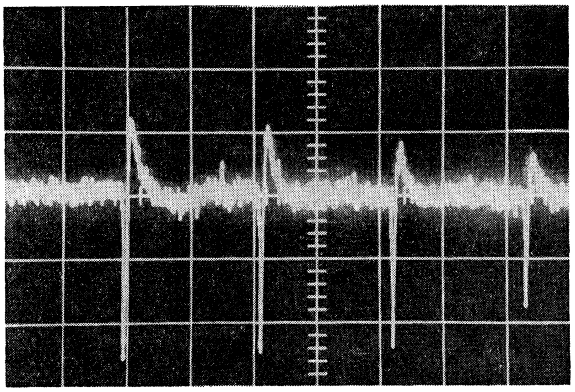

FIG. 12. The rf Zeeman transitions in polarized Na for the situation where the spin-exchange time is approximately the same as the spin-relaxation time. The four Zeeman transitions in the $F=2$ state are clearly visible but the Zeeman transitions in the $F=1$ state are smaller than the noise. The cell used contained He buffer gas whose density was 1.62×10^{17} atoms/cc. The temperature of the cell was 138°C. Because the spin-relaxation time was short the signals were weak and some narrow banding was used. This narrow banding caused the signals to appear as sharp spikes with a longer overshoot.

are given in Table VI. These state populations were calculated assuming the resonance radiation was left circularly polarized D_1 radiation only and that the intensity of the light was low. The other assumptions upon which these calculated populations are based are discussed in the Appendix. Since the populations of the three sublevels are the same in the $F=1$ state, δ must be equal to zero. Using this and the extrapolated value of $T_1=16$ msec the value of the spin-exchange collision time can be calculated. This is 5 msec. The spin-exchange cross section found from this measurement is given in Table V. This measurement may be somewhat in error because the light intensity was not low enough

for the calculated populations to be correct or because the other assumptions upon which the calculations were made were not satisfied.

IV. CONCLUSIONS

The measurements reported in this paper on the spin-relaxation times of optically oriented sodium diffusing in helium and neon buffer gases have revealed very long relaxation times at high buffer gas densities. This is because the cross section for a disorienting collision of the sodium with a helium or neon atom is very small. These cross sections are smaller than the corresponding ones for rubidium,[1,2] and are the same order of magnitude as the cross section for sodium in argon.[5]

The measurements and analysis of the signal intensities and line shapes in an optically pumped system have given values of the spin-exchange collision times and an understanding of the role of spin-exchange collisions in establishing the state populations in this system. The spin-exchange cross sections obtained from these experiments are somewhat smaller than those previously reported for sodium but the errors in these cross sections may be large.[6,13] Those effects which depend only on the general features of the spin-exchange collisions are explained very well by the analysis presented.

ACKNOWLEDGMENTS

We should like to thank Professor F. M. Pipkin of Harvard University for the generous loan of the Lyot polarization filter.

APPENDIX

A question, which has not yet been discussed, is whether the decay observed and discussed in the first section of this paper represents the spin-lattice relaxation time of the sample. Although no answer is easily given to this question some comments on the problem will be presented in this Appendix.[22]

Suppose the population of a sublevel of the ground state of the sodium ensemble is given by n_i where the subscript i can represent any of the eight sublevels. The equation for the rate of change of any state population is given by $dn_i/dt=D\nabla^2 n_i-kn_i+\frac{1}{8}\sum_i kn_i+$spin-exchange collision terms where $n_i=n_i(r,\vartheta,\varphi,t)$, D is the diffusion constant and $k=N\bar{v}_{\rm rel}\sigma$. The spin-exchange terms can be found in Ref. 6. In this equation use has been made of the assumption that in a depolarizing collision of a sodium atom with a buffer gas atom the sodium atom is scattered with equal probability into all eight magnetic sublevels. These eight equations, also, have a subsidiary condition imposed on them which is that the total number of particles is constant, i.e., $\sum_i \int(dr)^3 n_i=1$. By definition $P=\sum_i m_i n_i$, so that $dP/dt=D\nabla^2 P-kP$, since $\sum_i m_i=0$ and since the spin-exchange terms cannot affect the polarization. That the polarization be zero at the wall is a boundary condition.

The absorption in the cell is $K=\sum_i AP_i n_i$, where A is a constant proportional to the light intensity, and P_i is the relative probability of absorption of the sublevel i of the ground state. The values of P_i are given in Table IV. A method of writing the values of P_i given in Table IV is $P_i=4\langle\frac{1}{2}-S_z\rangle_i$, as can be seen by evaluating $\langle S_z\rangle_i$ for each of the eight sublevels of the ground state. The absorption is therefore

$$K=\sum_i A' n_i\langle\tfrac{1}{2}-S_z\rangle_i=\tfrac{1}{2}A'-A'\sum_i n_i\langle S_z\rangle_i.$$

The absorption is not proportional to

$$P=\sum_i n_i\langle F_z\rangle_i=\sum_i m_i n_i,$$

but instead to $\sum_i n_i\langle S_z\rangle_i$, and hence the absorption will not obey the same equation of motion as the polarization of the sample because the spin-exchange terms will make a nonvanishing contribution. It is probable, therefore, that the observed decay and analysis give approximate values for the diffusion constant and the cross section for disorientation but not precise values.

Of course, the equation for the rate of change of the various state populations for an optically oriented vapor given previously in Ref. 6,

$$\begin{aligned} dn_i/dt=&-AP_i n_i+\tfrac{1}{8}\textstyle\sum_j AP_j n_j-\dfrac{(n_i-\frac{1}{8})}{T_1}\\ &+\bar{v}_{\rm rel}\sigma_0\{\sum_{k,l,m} n_k n_l|(i;m|P_1\\ &+e^{-i\phi_{ts}}P_0|k;l)|^2{}_{\text{av over }\phi_{ts}}\\ &-\sum_{k,l,m} n_i n_m|(k,l|P_1\\ &\qquad +e^{-i\phi_{ts}}P_0|i,m)|^2{}_{\text{av over }\phi_{ts}}\},\end{aligned}$$

also has many assumptions in it which are not precisely correct. Some of these approximations are that n_i is independent of the spatial coordinates, that a single relaxation time T_1 can represent the diffusion of the sodium to the wall and disorientating collisions of the sodium with the buffer gas, that the constant A is independent of wavelength, that the cell is optically thin, that the reorientation of the sodium is complete in the excited P state, and that the spin-exchange collisions can be represented by an average relative velocity $\bar{v}_{\rm rel}$ and an average cross section σ_0. Because these assumptions are not exactly correct and because of the

[22] A. L. Bloom, Phys. Rev. **118**, 664 (1960). This paper contains an excellent discussion of the difficulty of attempting to interpret the observed decay of the optical signal as the relaxation time of the sample. It treats several possible interactions and does not assume that the disorienting collisions of the sodium with the buffer gas must scatter the sodium with equal probability into all other states. The conclusion reached by Bloom is that the observed signal in an experiment using Franzen's method is not simply related to the spin-relaxation time.

difficulties discussed in the main body of the paper a calculation of the intensities of the Zeeman rf transitions in the general case is very difficult. Hence, the spin-exchange collision times obtained from the measured intensities cannot have great accuracy.

The measurements of the spin-exchange collision time based on the line shape when the static magnetic field is swept rapidly are free of these assumptions as are the measurements on the state populations when the spin-exchange collision time is short compared to the spin relaxation time or the pumping time. These measurements depend only on the general features of the spin-exchange collisions discussed in the main body of the paper.

PHYSICAL REVIEW VOLUME 132, NUMBER 2 15 OCTOBER 1963

Hyperfine Structure and Nuclear Moments of Promethium-147 and Promethium-151*

BURTON BUDICK† AND RICHARD MARRUS
Lawrence Radiation Laboratory, University of California, Berkeley, California
(Received 3 June 1963)

The atomic-beam magnetic-resonance method has been used to measure the hyperfine structure of the $^6H_{7/2}$ level in two promethium isotopes. The spins of these isotopes have been verified to be $I(\mathrm{Pm}^{147})=\frac{7}{2}$ and $I(\mathrm{Pm}^{151})=\frac{5}{2}$. The electronic splitting factor (g_J) has been measured for the $^6H_{7/2}$ level and is found to be $g_J=-0.8279(4)$, in good agreement with the predicted value. The hyperfine constants and the nuclear moments inferred from them are found to be

for Pm^{147}: $|A|=447.1(9.3)$ Mc/sec, $|B|=267.5(70.8)$ Mc/sec, $B/A<0$,
$|\mu_I|=3.2(3)$ nm, $|Q|=0.7(3)$ b $Q/\mu>0$;

and

for Pm^{151}: $|A|=358(23)$ Mc/sec, $|B|=777(94)$ Mc/sec, $B/A<0$,
$|\mu_I|=1.8(2)$ nm, $|Q|=1.9(3)$ b, $Q/\mu>0$.

The nuclear moments are corrected for the breakdown of Russell-Saunders coupling. The stated errors include uncertainties in the fields at the nucleus arising from errors in the value of $\langle 1/r^3\rangle$ and the neglect of core polarization on the magnetic hyperfine structure. Corrections due to the Sternheimer effect have not been included. The measurements are shown to be consistent with the hypothesis that Pm^{147} is not highly deformed and can be understood from the shell model, but that Pm^{151} is highly deformed and must be interpreted by the collective model.

INTRODUCTION

IT is an experimentally well-established fact that collective effects become important in nuclei for neutron numbers N greater than about 88. The consequences of collective motion for the nuclear moments of a pair of isotopes can be very striking. An example, pertinent to our experiment, is the moments of Eu^{151} and Eu^{153} with neutron numbers 88 and 90, respectively. For Eu^{153}, which is highly deformed, the spectroscopic quadrupole moment is about twice that of Eu^{151}. Moreover, the measured magnetic moment of Eu^{153} is considerably less than that of Eu^{151}, and is one of the rare examples of a magnetic moment that lies in the wrong Schmidt group.[1]

For the pair of promethium isotopes under investigation here, the neutron numbers are 86 and 90. Part of the theoretical incentive for this work was to attempt to establish the onset of collective effects for N greater than 88 as valid for the isotopes of promethium. It will be seen shortly that our results are strikingly similar to those found in europium.

Earlier work on these isotopes had already established the spins and parities of the nuclear ground states. The spin of Pm^{147} had been shown[2] to be $\frac{7}{2}$ and that of Pm^{151} to be $\frac{5}{2}$.[3] If the nuclear core is unmodified by the addition of neutron pairs, the spins of a set of odd-Z isotopes should remain unchanged. Hence, the change in spin can be interpreted as evidence for the onset of collective motion.

Many workers have investigated the beta decay from the ground state of promethium-147 and have assigned positive parity to this state. The population of the energy levels of Pm^{151} by the beta decay of Sm^{151} has been investigated by Schmid and Burson.[4] They assign positive parity to the Pm^{151} ground state. In

* Work done under the auspices of the U. S. Atomic Energy Commission.

† Present address: Department of Physics, Columbia University, New York 25, New York.

[1] Maria Goeppert Mayer and J. Hans D. Jensen, *Elementary Theory of Nuclear Shell Structure* (John Wiley & Sons, Inc., New York, 1960).

[2] A. Cabezas, I. Lindgren, E. Lipworth, R. Marrus, and M. Rubinstein, Nucl. Phys. **20**, 509 (1960).

[3] A. Cabezas, I. Lindgren, and R. Marrus, Phys. Rev. **122**, 1796 (1961).

[4] L. C. Schmid and S. B. Burson, Phys. Rev. **115**, 178 (1959).

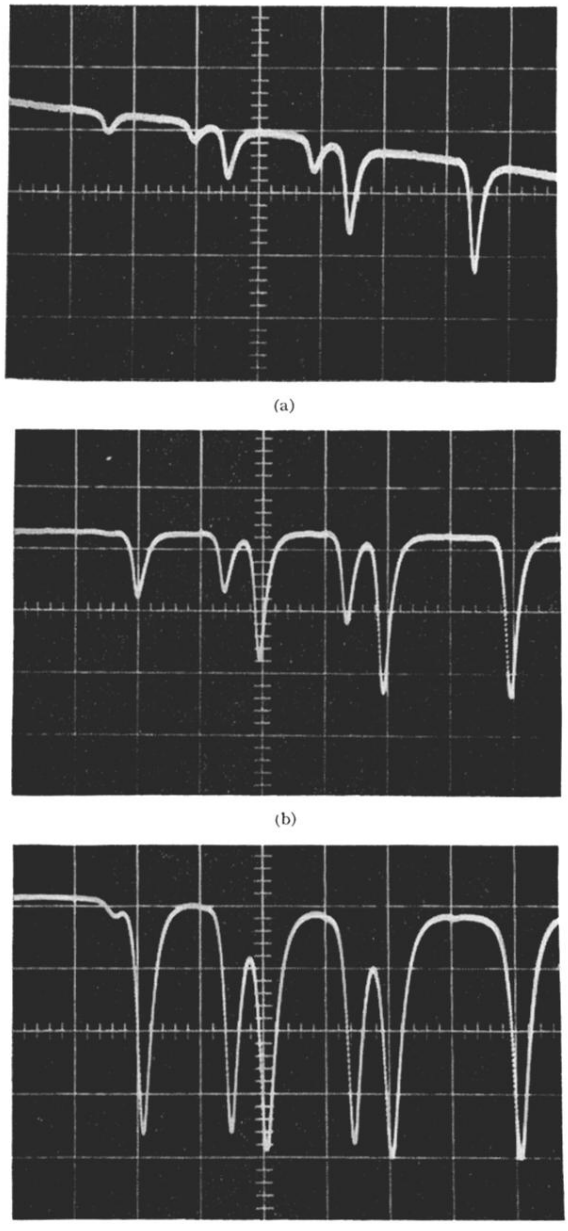

(a)

(b)

(c)

FIG. 11. The effect of the magnitude of the rf magnetic field on the Zeeman transition in polarized Na. The rf voltage levels as measured at the generator were in the ratio 1:4:8 for pictures (a), (b), and (c), respectively. The signal strength increases with the rf level; the vertical scales were 2, 2, and 5 mV/div for pictures (a), (b), and (c), respectively. These pictures were taken using a cell whose density was 2.4×10^{19} He atoms/cc and whose temperature was 195° C. The sweep speed of the static magnetic field was 5 sec/div.

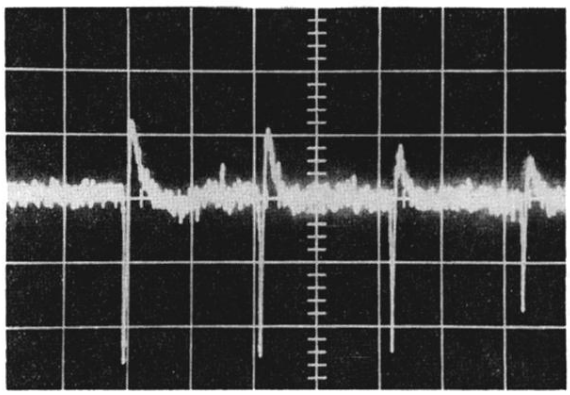

FIG. 12. The rf Zeeman transitions in polarized Na for the situation where the spin-exchange time is approximately the same as the spin-relaxation time. The four Zeeman transitions in the $F=2$ state are clearly visible but the Zeeman transitions in the $F=1$ state are smaller than the noise. The cell used contained He buffer gas whose density was 1.62×10^{17} atoms/cc. The temperature of the cell was 138°C. Because the spin-relaxation time was short the signals were weak and some narrow banding was used. This narrow banding caused the signals to appear as sharp spikes with a longer overshoot.

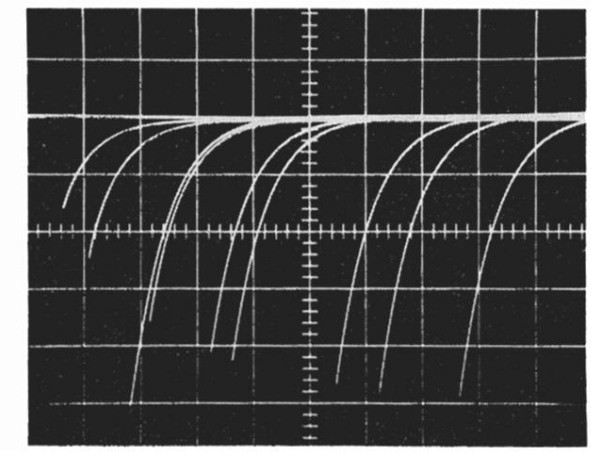

FIG. 2. The decay of the cell transparency. Time increases from left to right in units of 500 msec/div. The photocell output increases from bottom to top in units of 50 mV/div. The long trace two units from the left is a reference showing the transparency of an unpolarized cell. This picture was taken with the cell at a temperature of 173°C and using a cell whose density was 1.63×10^{19} He atoms/cc.

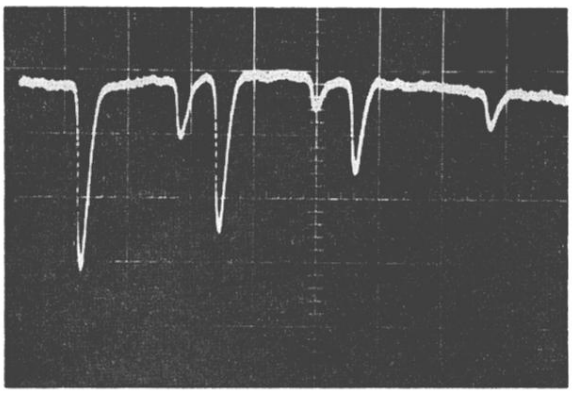

FIG. 7. The rf-induced Zeeman transitions in a polarized Na sample. The magnetic field increases from left to right at a rate of 5 sec/div. The output of the photocell increases from bottom to top in units of about one mV/div. The rf field was small enough that saturation was negligible. The oscillator frequency was approximately 9.8 Mc/sec. The cell used had a density of 1.15×10^{19} He atoms/cc and the temperature was 135°C.

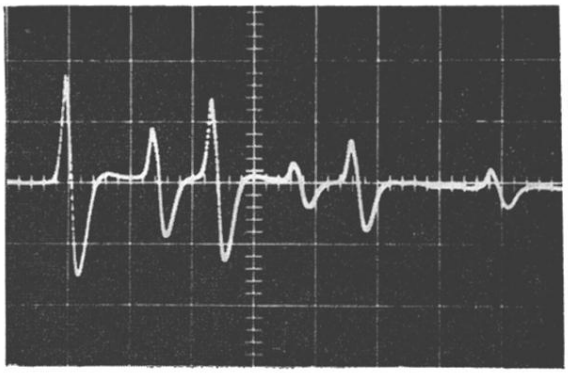

(a)

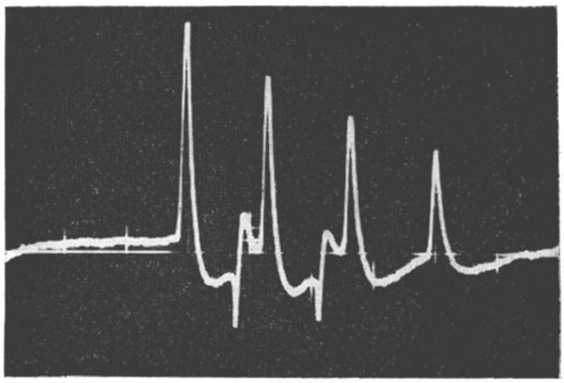

(b)

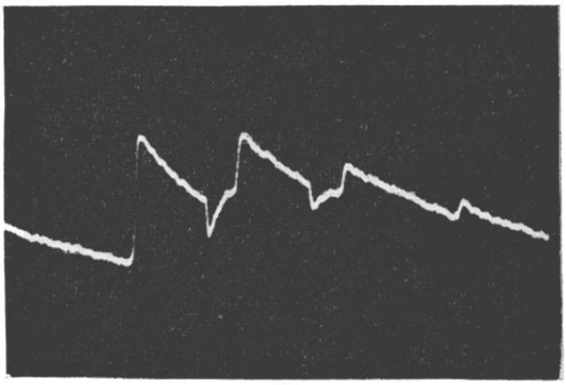

(c)

FIG. 8. The Zeeman transitions in polarized Na, showing the effect of the rate at which the magnetic field is swept across the resonance. The magnetic field increases from left to right. The oscilloscope was ac coupled to the photocell, giving a derivative-type line shape. Reading from the left, the second and fourth resonances are the Zeeman transitions in the $F=1$ hyperfine state. The sweep speed of the magnetic field for the three pictures was 2 sec/div for picture (a), 200 msec/div for picture (b), and 50 msec/div for picture (c). In picture (a) the resonances all have the same general shape of the absorption followed by an RC undershoot (increased absorption caused a bottom to top deflection of the trace). In picture (b) the two Zeeman resonances in the $F=1$ state have the initial spike of lower absorption followed by increased absorption. In picture (c) the sweep is rapid enough that the light does not pump the system back to equilibrium before the next resonance is reached. In picture (c) the two Zeeman resonances in the $F=1$ state correspond to lower absorption for the cell and the sweep is rapid enough that the shape of the spike is shown. The pictures (a), (b), and (c) are shown only to explain the effect and were not all taken on the same cell or at the same temperature.